STABILIZATION OF THE COLLAGEN TRIPLE HELIX WITH A RUTHENIUM(II) ANCHOR

by

Patrick Banzon

A Senior Honors Project Presented to the

Honors College

East Carolina University

In Partial Fulfillment of the

Requirements for

Graduation with Honors

by

Patrick Banzon

Greenville, NC

May 2017

Approved by:

William E. Allen, PhD

Department of Chemistry

Thomas Harriot College of Arts and Sciences

ABSTRACT

Two collagen analogues based on a $(Pro\text{-}Hyp\text{-}Gly)_7$ core were given metal-binding ability by linking histidine to either the *N*- or *C*- termini using a six-carbon spacer. Circular dichroism studies confirmed that the isomers, dubbed HPOG and POGH, form triple-helices which cooperatively unwind at T_m = 34.8 and 35.6 °C, respectively. Three strands of the HPOG peptide were bound to a ruthenium ion, by heating in the presence of tris(pyrazol-1-yl)borato ruthenium(II) (Tp-Ru). The strands of the *N*-Anchored complex unwind at a temperature about 10 °C higher, but do so over a broader temperature span. Thus, immobilization of collagen on a metal ion hub appears to increase helix stability while decreasing cooperativity of folding/unfolding. DFT calculations suggest that the loss of cooperativity arises from the disruption of interstrand hydrogen bonding. Other spacer groups, or other metal ions, may be necessary to promote optimal approach of strands to each other.

TABLE OF CONTENTS

LIST OF FIGURES

LIST OF SCHEMES

LIST OF ABBREVIATIONS

In Alphabetical Order:

Ac: Acetyl Group

Ahx: 6-ε-Aminohexanoic Acid

C-Anchored: Tp-Ru[Ac-(Pro-Hyp-Gly)$_7$-Ahx-His-NH_2]$_3$

CRP: Collagen Related Peptide

DFT: Density Functional Theory

ESI+: Electrospray Ionization

Gly: Glycine

His: L-Histidine

HPOG: Ac-His-Ahx-(Pro-Hyp-Gly)$_7$-NH_2

Hyp: Hydroxyproline

MALDI: Matrix-Assisted Laser Desorption/Ionization

N-Anchored: Tp-Ru[Ac-His-Ahx-(Pro-Hyp-Gly)$_7$-NH_2]$_3$

PBS: Phosphate Buffered Saline

POGH: Ac-(Pro-Hyp-Gly)$_7$-Ahx-His-NH_2

Pro: Proline

Tp-Ru: Tris(pyrazol-1-yl)borato ruthenium(II)

CHAPTER 1: INTRODUCTION

1.1: Protein/Polypeptide Structure

Proteins are macromolecules with massive sophistication and utility. The many roles proteins play in life processes[1,2] depend on their structures, which are determined, in part, by two local criteria: rotational freedom of amino acid side-chains and maximizing of hydrogen-bonds.[3] This thesis is focused on the structure of collagen, the most abundant protein in mammals.[4] Collagen shows great rigidity because it is rich in the amino acid proline (Pro, P), the most conformationally restricted amino acid, and because it forms thousands of H-bonds between its three component polypeptide strands.[4]

Side-chains have unique properties that allow proteins to respond to their environment. Maximal side-chain motions (with high entropy) are likely, for example, when a hydrophilic protein is in an extended conformation, fully solvated by water; lesser freedom of movement results when a protein collapses upon itself to bury hydrophobic surfaces away from water. This folding phenomenon is inhibited when the protein experiences steric hindrance. When bulky backbones discourage attempts at lowering entropy, an energetic "tug-of-war" occurs.[1]

Continuing this "yin-yang" effect, optimizing of hydrogen-bonding also competes with side-chain conformational entropy. The attractive local interactions in hydrogen-bonding can often compensate for lowering of entropy. The opposite effect is just as plausible, however, where enthalpy is favored over entropy. Altogether, to anticipate native secondary structure, both factors must be considered.[2,5]

1.2: The Collagen Triple-Helix

In 1940, Astbury & Bell proposed that collagen consists of a single extended polypeptide chain.[6] In 1951, Pauling & Corey proposed the α-helix and β-sheet, and a paradigm shift in collagen research took place.[7] From then on, it was suspected that multiple polypeptide strands were held together by hydrogen bonding. In 1954, Ramachandran & Kartha used fiber diffraction data to propose a triple-helical structure.[8] It consisted of three staggered, left-handed polyproline helices within an overall right-handed helix, with *trans* peptide bonds and two hydrogen bonds per proline-hydroxyproline-glycine (Pro-Hyp-Gly, POG) triplet.[9] In 1955, Rich & Crick further refined the model. The modern view has a single interstrand N–H(Gly)···O=C(Xaa) hydrogen bond per triplet (Figure 1.1).[10]

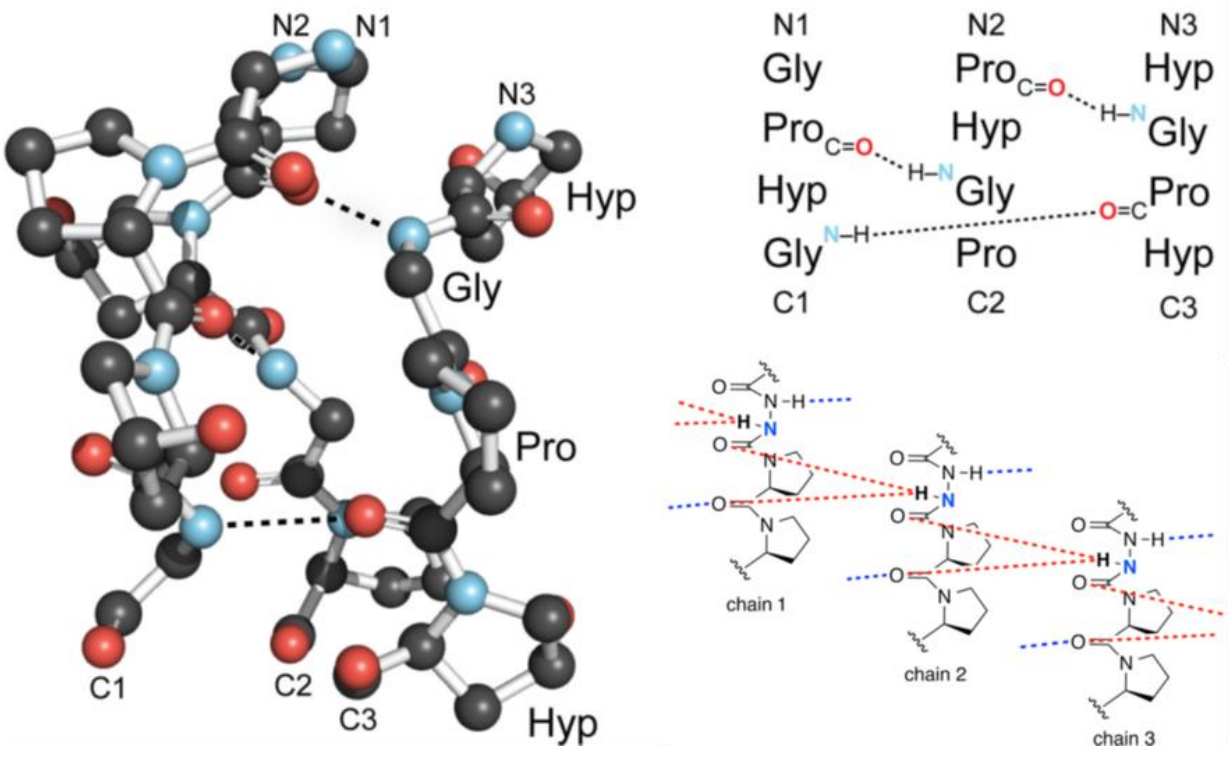

Figure 1.1: Ball-and-Stick Model of a Collagen Segment with Strand Bond Diagrams.

1.3: Applications of Collagen

Collagens are deposited in the extracellular matrix, then further supramolecular assembly takes place, so structural and mechanical support is provided to tissue formation.[1] Biological functions in the human body like skin cell replacement require the presence of collagens. They interact with cells via several receptor families that regulate cell proliferation, migration, and differentiation.[11]

Collagen is a highly adaptable material that is extensively used in the medical, dental, and pharmacological fields. The biocompatibility of metallic implants is improved with the presence of collagen, for example.[12,13] It can be formed into fibers, compacted solids, or gels,[11,14] each of which has medical applications. Resorbable forms of collagen can dress oral wounds, graft closures, and extraction sites to promote healing.[15] Clinicians have used exogenous collagen in periodontal and implant therapy as barriers to prevent epithelial migration and to allow cells with regenerative capacity to repopulate the defect area.[15]

1.4: Stabilizing the Triple Helix: Hypothesis

In clinical treatments where exogenous collagen is introduced into the body, such as tissue augmentation, drug delivery, and bone grafts, improvement in its biocompatibility and resistance to degradation are greatly desired.[16] Just as the ends of a rope are susceptible to fraying, degradation of collagen begins when its strands unwind. Recent attempts to strengthen the triple-helix of collagen via backbone and side chain modification[17,18] have often decreased its stability instead. Certain exceptions are peptoid residue substitution, fluorination of prolines, and aza-glycine substitution (Figure 1.2).[17,18,19] These specific modifications have made the helix

more resistant to denaturation, as judged by melting temperature T_m, while maintaining a level of cooperativity similar to that of the native protein. A combination of all these modifications can lead to massive hyperstability of the collagen triple-helix.[19]

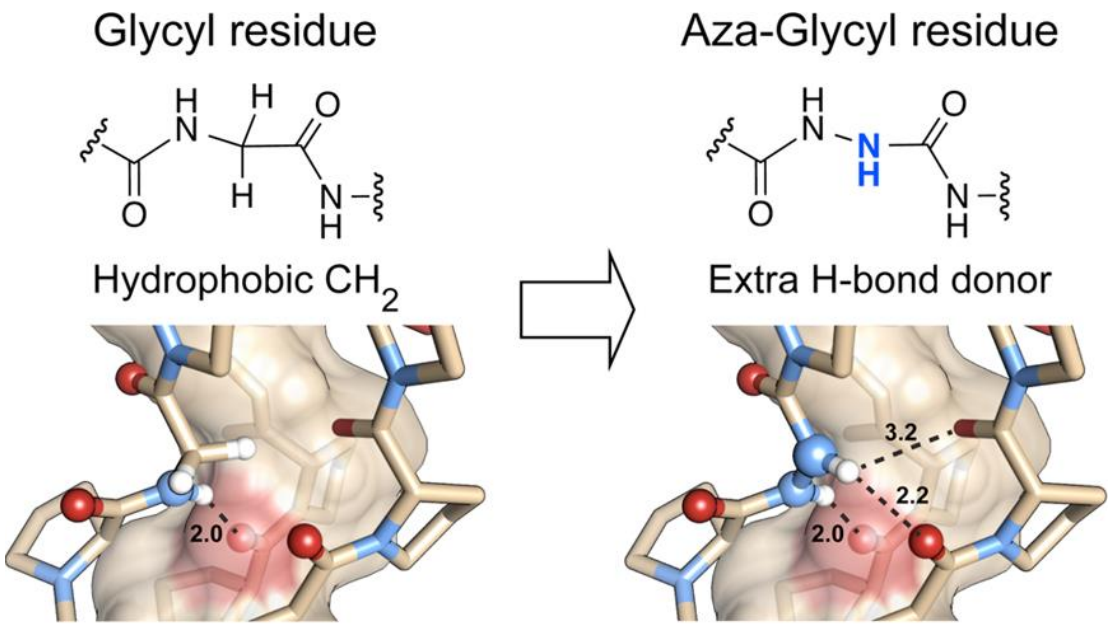

Figure 1.2: Structure of a Collagen Analogue Containing aza-Gly.[18]

Described here is a different approach to stabilizing collagen. Instead of modifying the amino acid building blocks themselves, a metal ion was added to the end of the three individual protein strands to prevent fraying (Figure 1.3). The presence of the metal complex was expected to protect the anchored terminus from protease enzyme degradation. However, it was recognized that the presence of the metal ion might prevent the strands from approaching each other in a favorable manner. The addition of a flexible non-natural amino acid was therefore explored, to allow the polypeptide subunits to adopt the correct "register," in which each strand is staggered by one residue. The complex was designed to prevent unwinding at

one end of the helix, comparable to an aglet preventing the threads in a shoelace from unraveling.

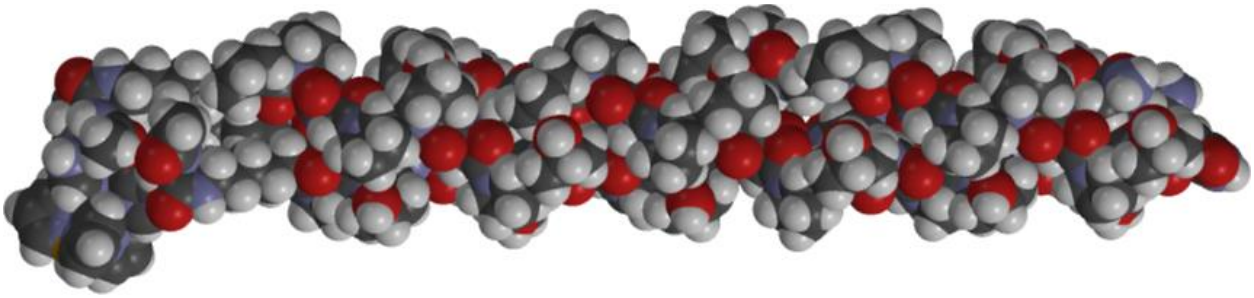

Figure 1.3: Space Filled Model of Secondary Structure of Collagen Tethered to an Anchor.

CHAPTER 2: SYNTHESIS OF AN *N*-ANCHORED COLLAGEN COMPLEX

2.1 Design of Peptides

To immobilize collagen on a metal ion hub, it must possess amino acid residues that can serve as ligands. Here, the *N*- and *C*-termini were the targeted sites of variation. A "link-and-spacer" motif was developed using two amino acids, histidine (His, H) and 6-ε-aminohexanoic acid (Ahx). Histidine possess an imidazole group, which is well-known to bind transition metals such as Cu(II) and Zn(II) in the active sites of enzymes. Unnatural 6-aminohexanoic acid provides flexibility for proper triple-helical formation, as the three peptides within the secondary structure are offset by one residue.[11] Therefore, this link-and-spacer could anchor individual collagen strands to a single point, yet allow enough fluid movement for the characteristic registry to be achieved.

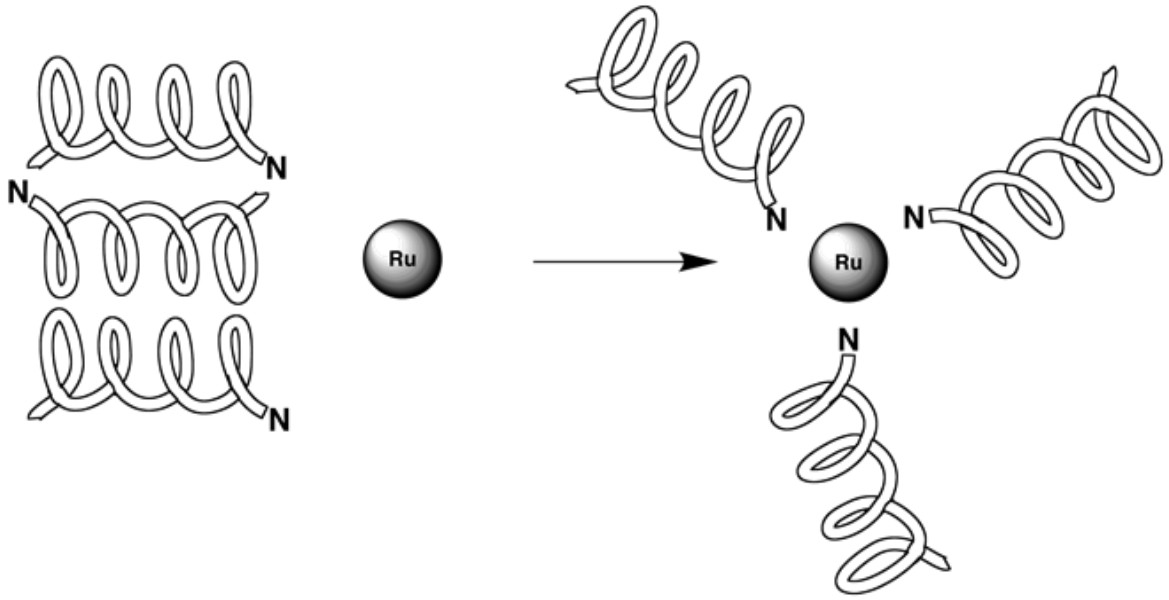

Figure 2.1: Simplified Blueprint of Link-and-Spacer Proposal.

Computational modeling predicted that close approach of individual collagen strands would be impossible without spacer groups. Simple Ac-His-Pro-NH_2 peptides lacking flexibility were complexed to the three vacant coordination sites of tris(pyrazol-1-yl)borato ruthenium(II) (Tp-Ru). High-level density functional theory (DFT) was used to generate two geometries that maximized hydrogen bonding at the *N*-termini or the imidazole rings (Figure 2.2). Relative energy values were 0.00 kcal/mol and 7.53 kcal/mol respectively. In both structures, the peptide fragments were found to be directed away from each other, preventing interactions between them.

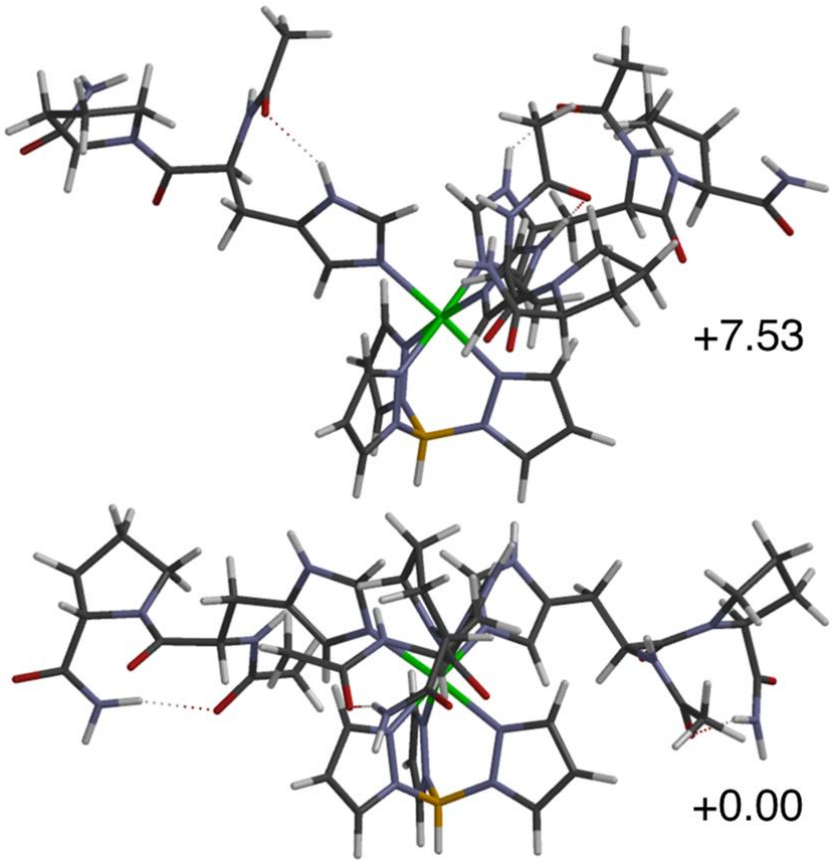

Figure 2.2 Preliminary Geometry Models of Anchoring Collagen Strands. Ru(II) = Green.

Subsequent computational studies demonstrated potential interstrand H-bonding when Ahx spacers were introduced between His and the (Pro-Hyp-Gly)$_n$ core. It is important to note that only two triplets of Pro-Hyp-Gly were modeled due to computational limitations. Inspection of *N*-anchored complex Tp-Ru[Ac-His-Ahx-(POG)$_2$-NH$_2$]$_3$ reveals fewer interstrand H-bonds than in the *C*-anchored isomer [Ac-(POG)$_2$-Ahx-His-NH$_2$]$_3$Ru-Tp (Figure 2.3); this is consistent with a higher relative energy value (+7.12 kcal/mol) for the former complex. Nonetheless, the modeling study suggests that the link-and-spacer unit is suited for coupling collagen at either end.

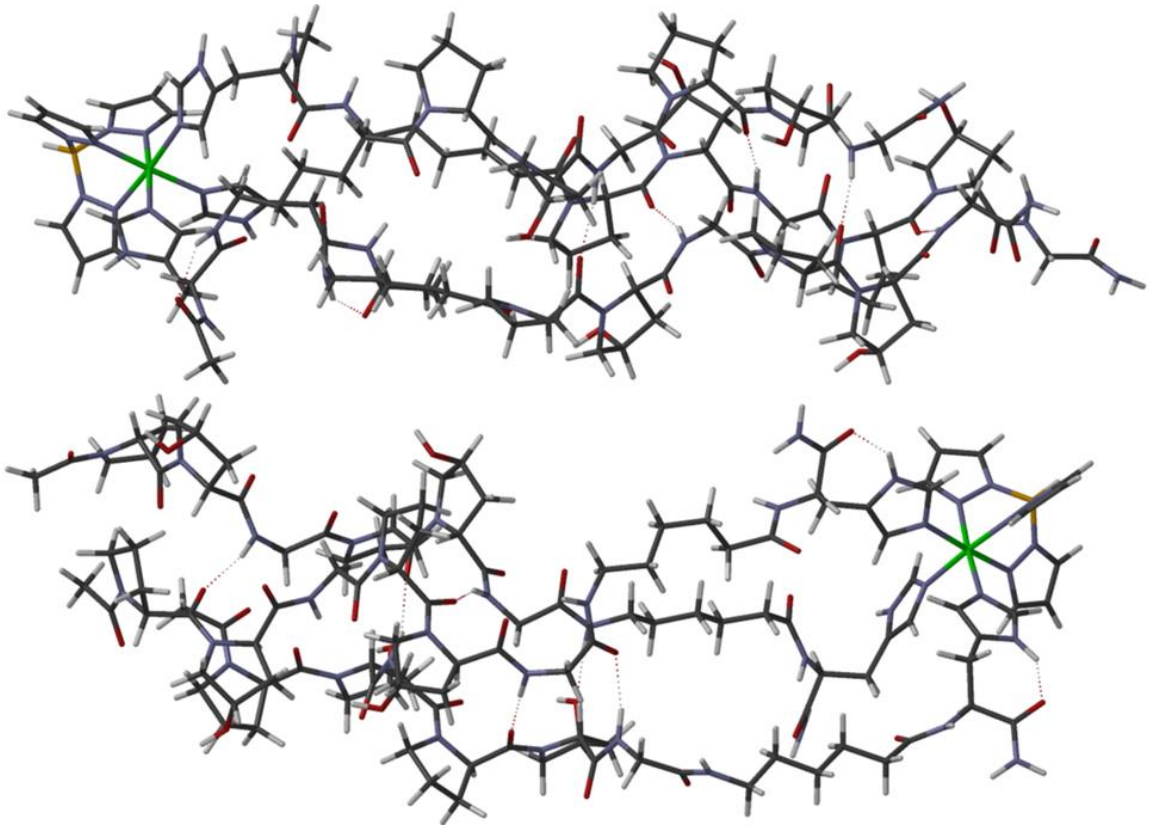

Figure 2.3: Predictions of Anchor Interactions with anchored *N*-terminus (top) and anchored *C*-terminus (bottom). Ru(II) = Green.

2.2 Synthesis of Collagen-Related Peptide (CRP) Isomers

Using standard Fmoc-based solid-phase peptide synthesis (SPPS), two isomeric collagen analogues possessing a $(Pro\text{-}Hyp\text{-}Gly)_7$ core, dubbed HPOG and POGH, were made. His-Ahx was assembled at the *N*-terminus of HPOG; Ahx-His was assembled at the *C*-terminus of POGH. Acetylation of the *N*-termini and amidation of the *C*-termini were performed to prevent unwanted side reactions.

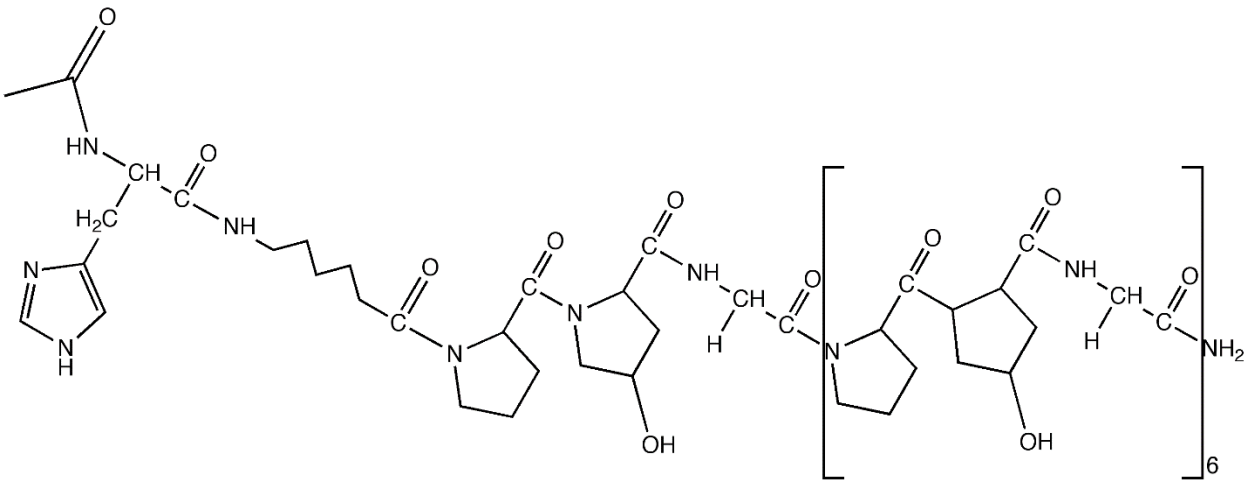

Scheme 2.1: Sequence of Ac-His-Ahx-(Pro-Hyp-Gly)$_7$-NH$_2$, dubbed HPOG.

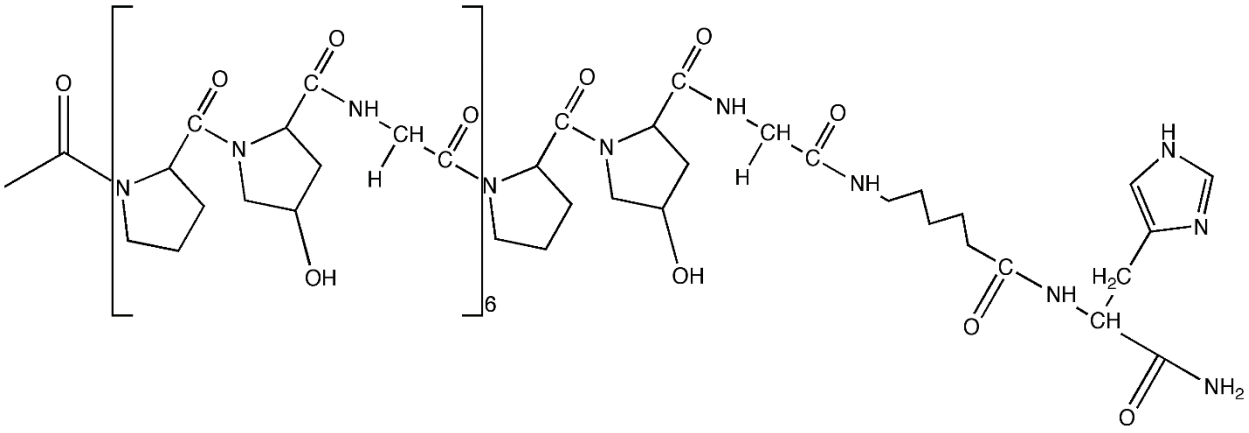

Scheme 2.2: Sequence of Ac-(Pro-Hyp-Gly)$_7$-Ahx-His-NH$_2$, dubbed POGH.

Once cleaved from the resin, the desired products were purified through reversed-phase HPLC with a water to acetonitrile gradient. Chromatograms of the crude cleavage products are shown below. After lyophilization, white feathery solids were obtained.

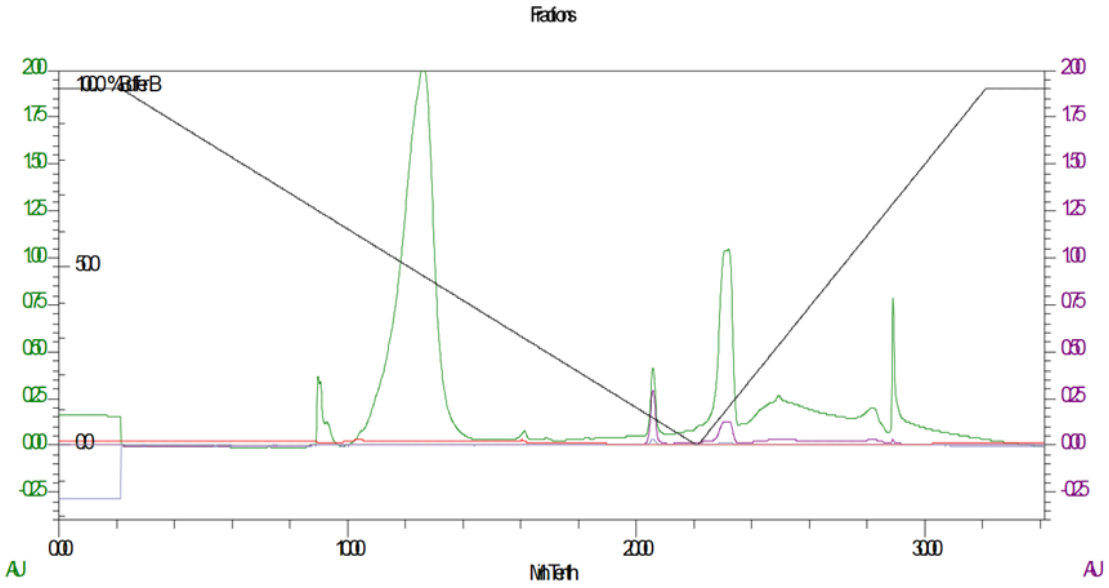

Figure 2.4: Preparative-Scale RP-HPLC Chromatogram of HPOG.

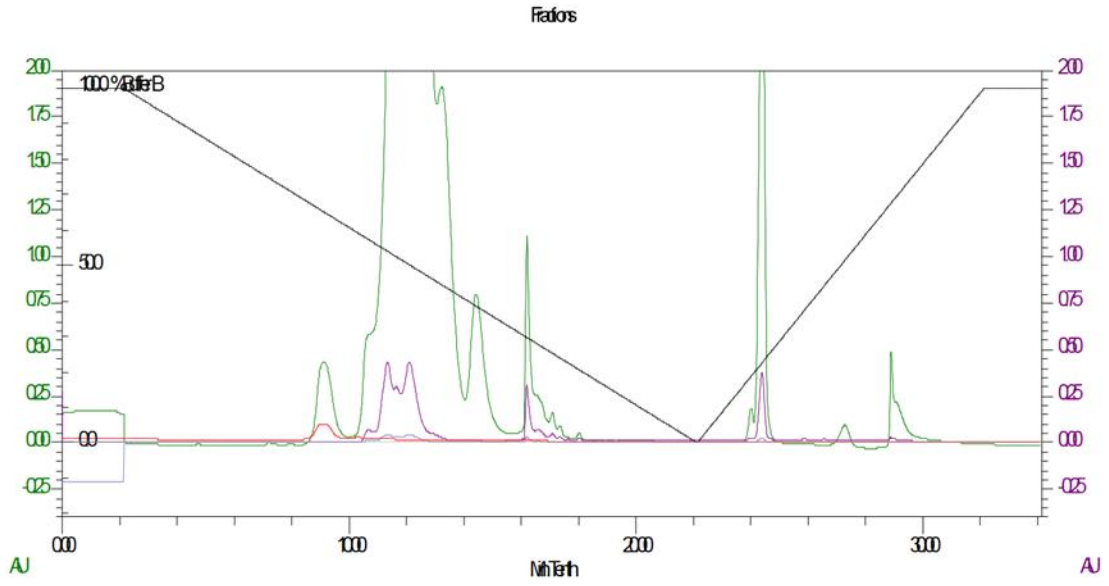

Figure 2.5: Preparative-Scale RP-HPLC Chromatogram of POGH.

2.3 Synthesis of Tp-Ru Anchor

An appropriate metal ion anchor should be stable in air and allow for coordination by exactly three CRP strands. Using ruthenium(II) in this role allows for an octahedral geometry, in

which 90° is the maximum separation between N atoms of the His residues. As an additional tridentate ligand, tris(pyrazol-1-yl)borate (Tp) occupies three coordination sites of Ru(II) in a facial (fac) manner. This orientation allows the CRP strands to attach closely to one another relative to the ruthenium atom.

Initial efforts to immobilize three HPOG strands onto commercially available Tp-$Ru(PPh_3)_2Cl$ failed, even under forcing conditions. Electrospray ionization mass spectrometry (ESI-MS) indicated that a triphenylphosphine ligand remained tightly bound to the Ru(II) center, preventing complete substitution by the collagen analogues. Therefore, a Tp-Ru starting material without PPh_3 was prepared. When heated under reflux in acetonitrile solvent, equal parts of potassium tris(pyrazolyl)borohydride (KTp) and ruthenium trichloride created a ruthenium(III) precursor to the desired Tp-Ru(II) product (Scheme 2.3). (Potassium iodide was present in the reaction mixture as well to serve as a potential reducing agent.) Note that although chloride and acetonitrile ligands are shown bound to Ru(III) in Scheme 2.3, the actual identities of the inner-sphere ligands are not known.

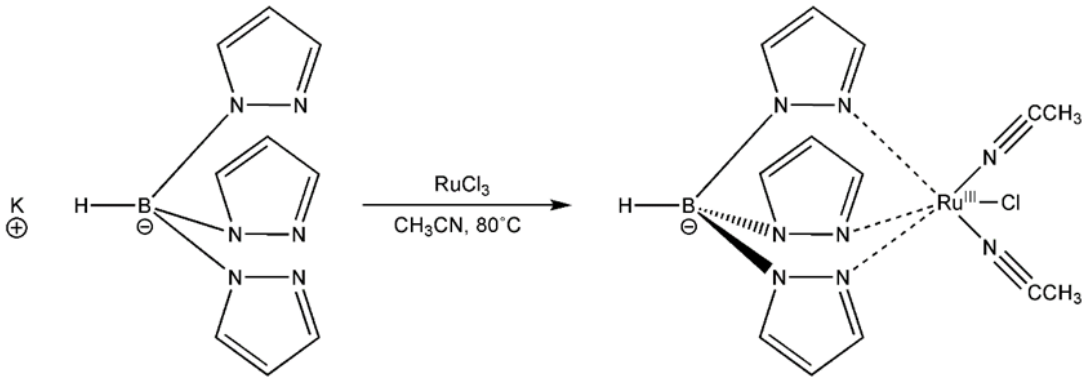

Scheme 2.3: Synthesis of Tp-Ru Complex.

The product created was a dark green solid that strongly adhered to glassware. Reduction of the green ruthenium(III) species was accomplished by heating equimolar amounts of the complex and sodium-L-ascorbate in a 5:1 acetonitrile:water (v:v) solvent mixture (Scheme 2.4). This reaction was run under a nitrogen atmosphere to minimize unwanted oxidation. The dark green mixture gradually turned light orange during reduction. Once the reaction had cooled to room temperature, similar HPLC conditions as mentioned previously were used to isolate a broad peak which absorbed at 360 nm. After lyophilization, a sticky reddish-brown solid was obtained.

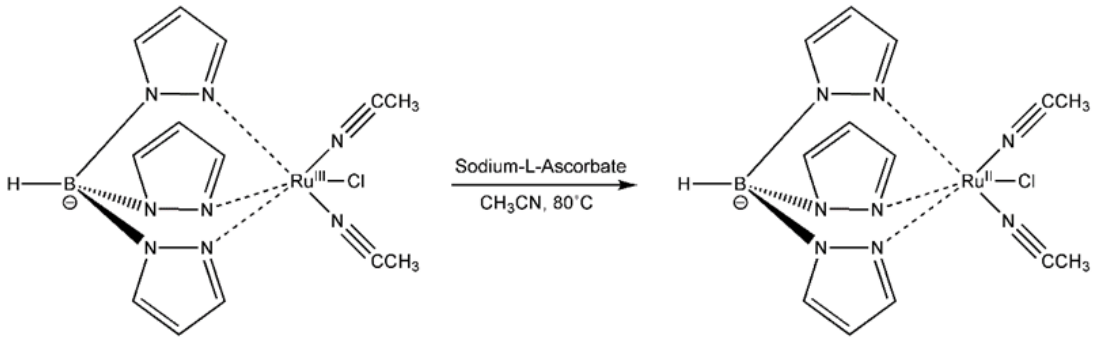

Scheme 2.4: Reduction of Tp-Ru Complex.

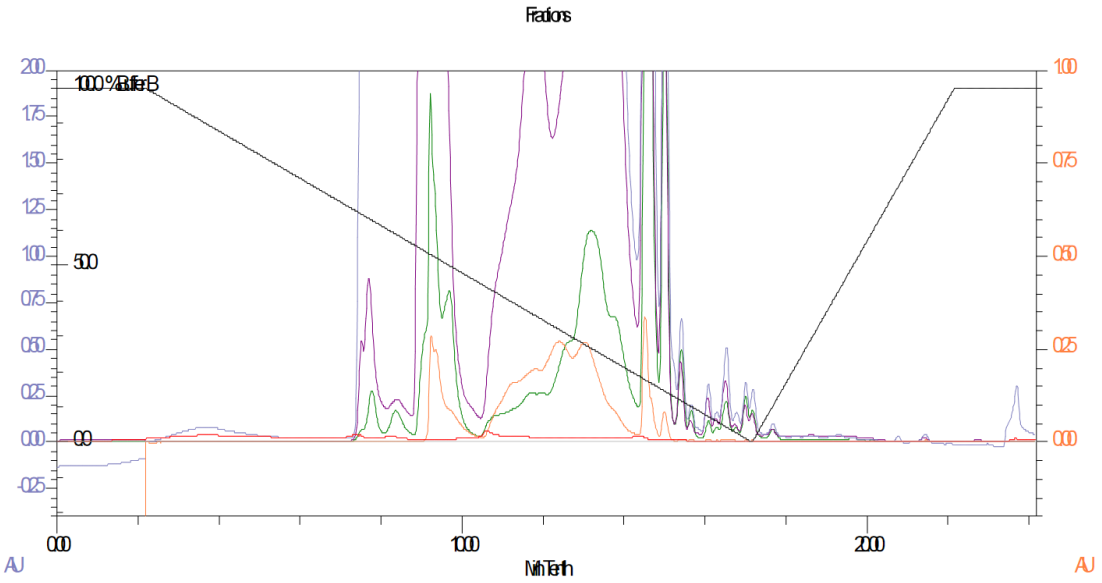

Figure 2.6: Preparative Scale RP-HPLC Chromatogram of Reduced Tp-Ru.

2.4 Synthesis of *N*-Anchored Complex

Once the anchor and CRP strands were prepared, suitable reaction conditions were planned to ensure substitution of the three coordination sites within Tp-Ru. HPOG and Tp-Ru were mixed in ethanol:water (1:1, v:v), then heated at reflux for 72 hours in the presence of a trialkylamine base. An excess of the peptide (3.5 equiv) was used to take advantage of Le Chatelier's principle (Scheme 2.5).

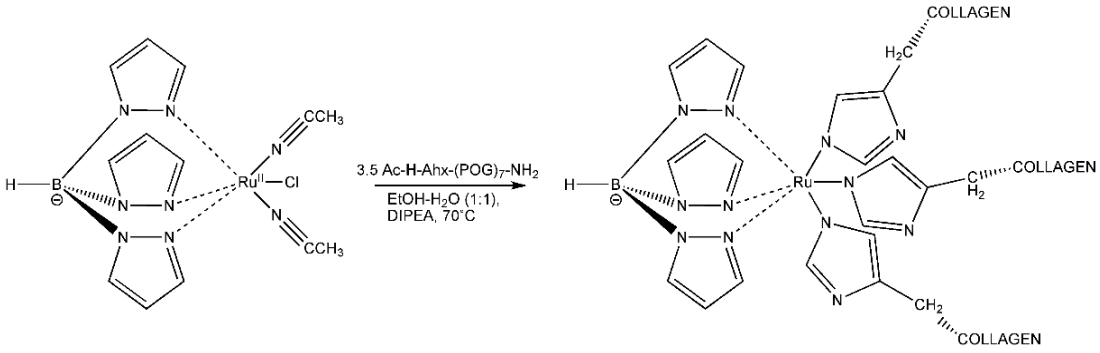

Scheme 2.5: Synthesis of *N*-Anchored Complex.

Once the reaction had cooled to room temperature, purification by RP-HPLC was performed using conditions similar to those above. One prominent peak with a UV-vis absorption at 360 nm was collected (Figure 2.7). The fraction was lyophilized to a light brown solid. Typically, ESI-MS would be used to confirm the mass (6835.12 g/mol) but the departmental instrument was out of operation at the time of this synthesis. Proton NMR integrations were consequently used to determine if three HPOG strands were present per Tp-Ru unit. A small amount of the lyophilized product was dissolved in DMSO-d_6. Integrations at 8.95 and 8.35 ppm were consistent with the binding of three CRP strands onto Tp-Ru (Figure 2.8).

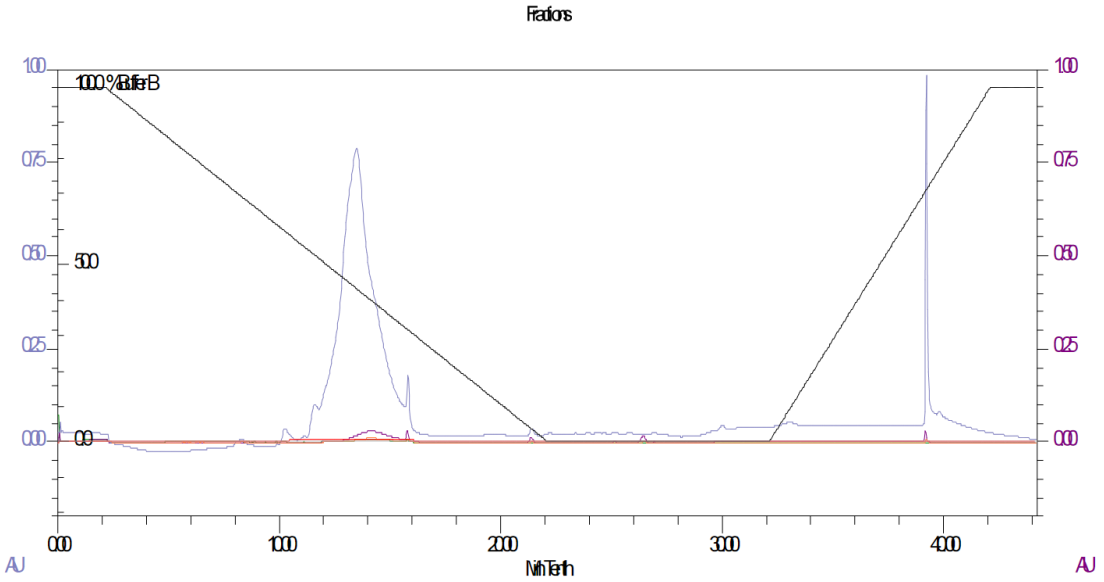

Figure 2.7: Preparative Scale RP-HPLC Chromatogram of *N*-Anchored HPOG.

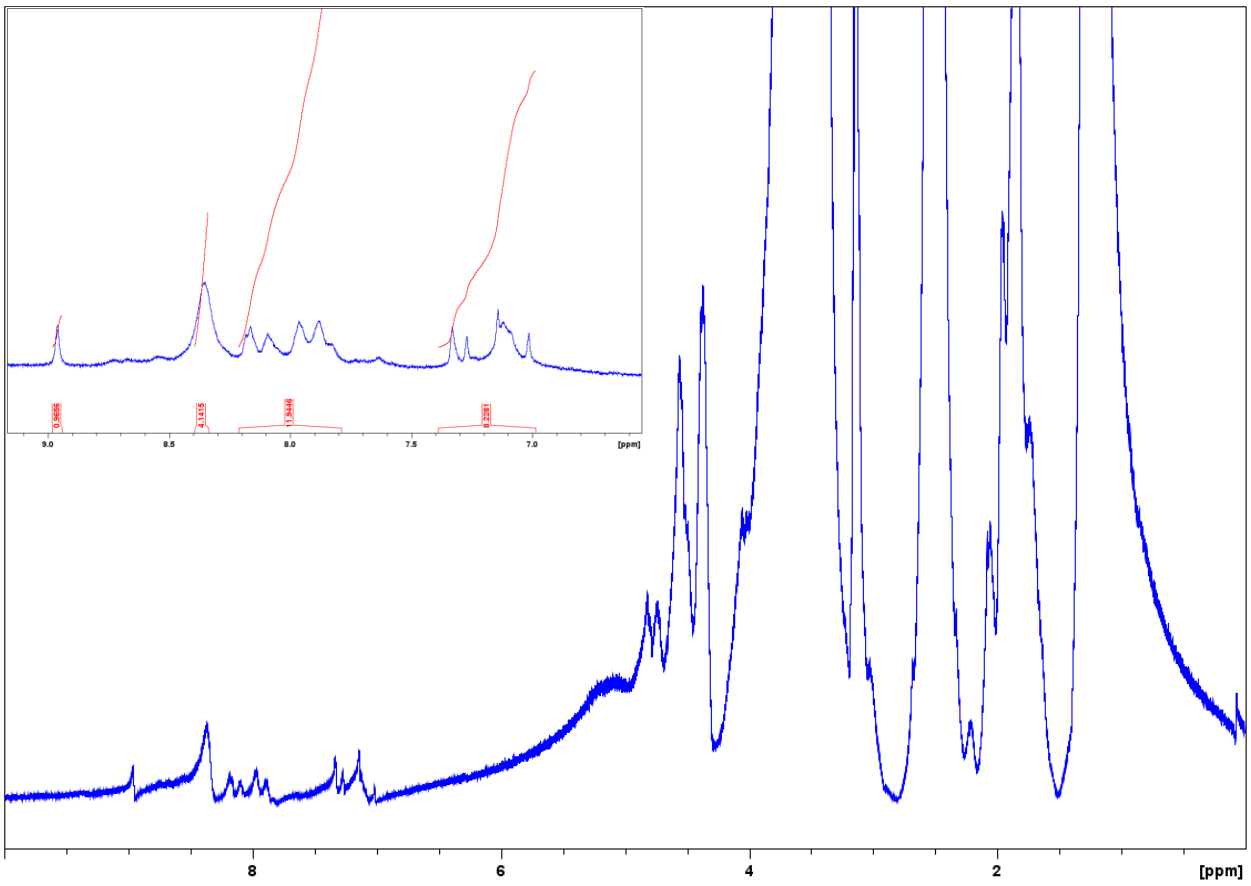

Figure 2.8: Proton NMR Spectrum of *N*-Anchored HPOG.

CHAPTER 3: THERMAL DENATURATION STUDIES

3.1 CRP Isomer Studies

Circular dichroism (CD) spectroscopy was applied to study the secondary structures of HPOG, POGH, and the *N*-Anchored ruthenium complex. In previous work by the Chenoweth group, CD studies showed that introduction of aza-Gly into $(POG)_7$ analogues increases the temperature at which the triple-helix unfolds.[18,19] The CRP isomers HPOG and POGH were diluted to a concentration of 0.20 mM in PBS solution for comparison. Both isomers exhibited maxima at 225 nm at 15 °C, indicative of triple-helix formation.

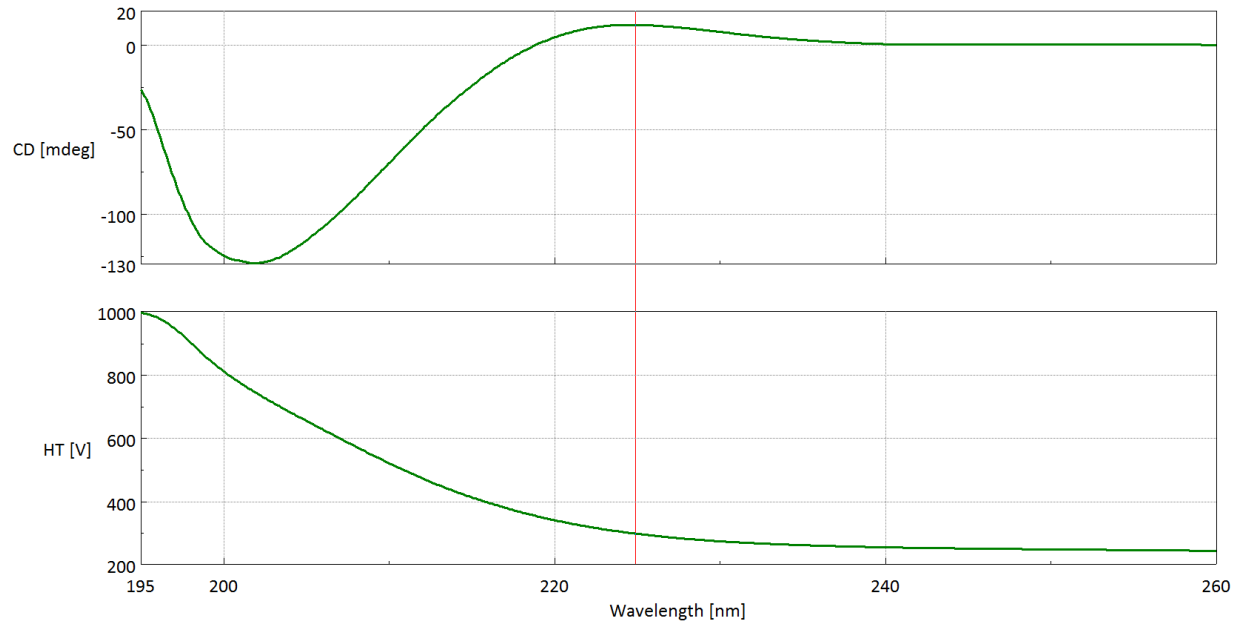

Figure 3.1: CD Spectrum of HPOG at 15 °C.

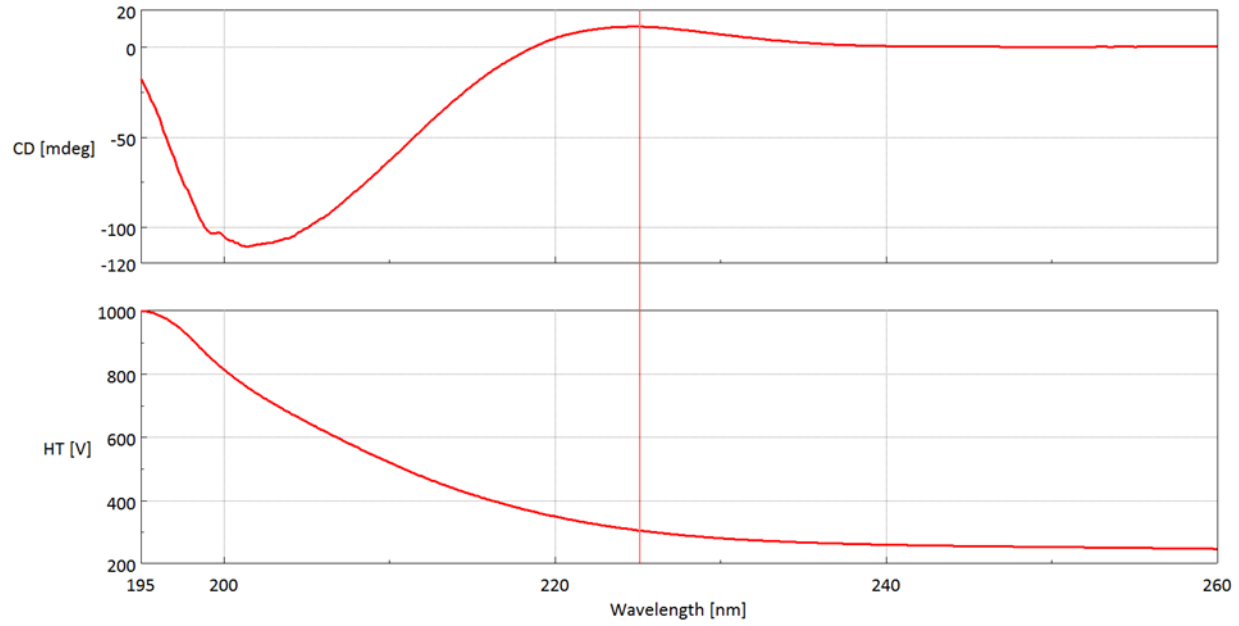

Figure 3.2: CD Spectrum of POGH at 15 °C.

Thermal denaturation studies with temperature gradients of 36 °C/hour and 12 °C/hour revealed cooperative unfolding like that reported by Chenoweth.[18] However, the presence of histidine and 6-aminohexanoic acid at either the *N*- or *C*- termini causes the $(POG)_7$ core to unfold at a lower temperature. The melting temperatures (T_m), at which 50% of structure is fully unfolded, are shown in the four figures below. The CD data were fit to a two-state model as reported by Vargas-Uribe et al.[20] The T_m for HPOG and POGH are 34.8 ∓ 0.2 °C and 35.6 ∓ 0.2 °C, respectively. The enthalpy values (ΔH) for HPOG and POGH are 33.2 ∓ 1.5 kcal/mol and 34.9 ∓ 2.8 kcal/mol. The higher T_m and ΔH of POGH follow the trends observed in the computational studies (Section 2.1). It thus appears that placing the link-and-spacer motif at the *C*-terminus of $(POG)_7$ causes less disruption to the helical core.

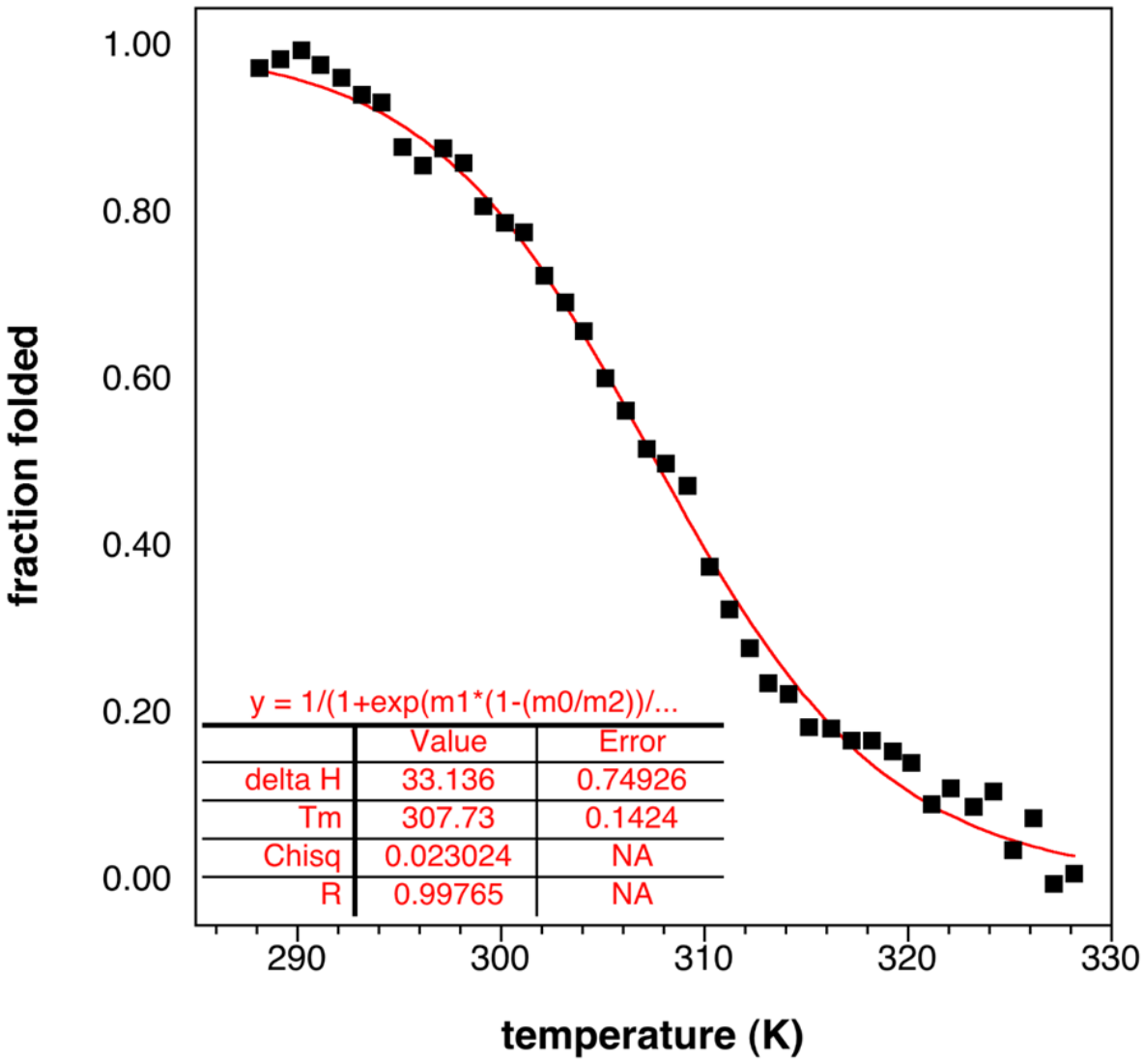

Figure 3.3: Melting Curve of HPOG at a 36 °C/hour Ramp.

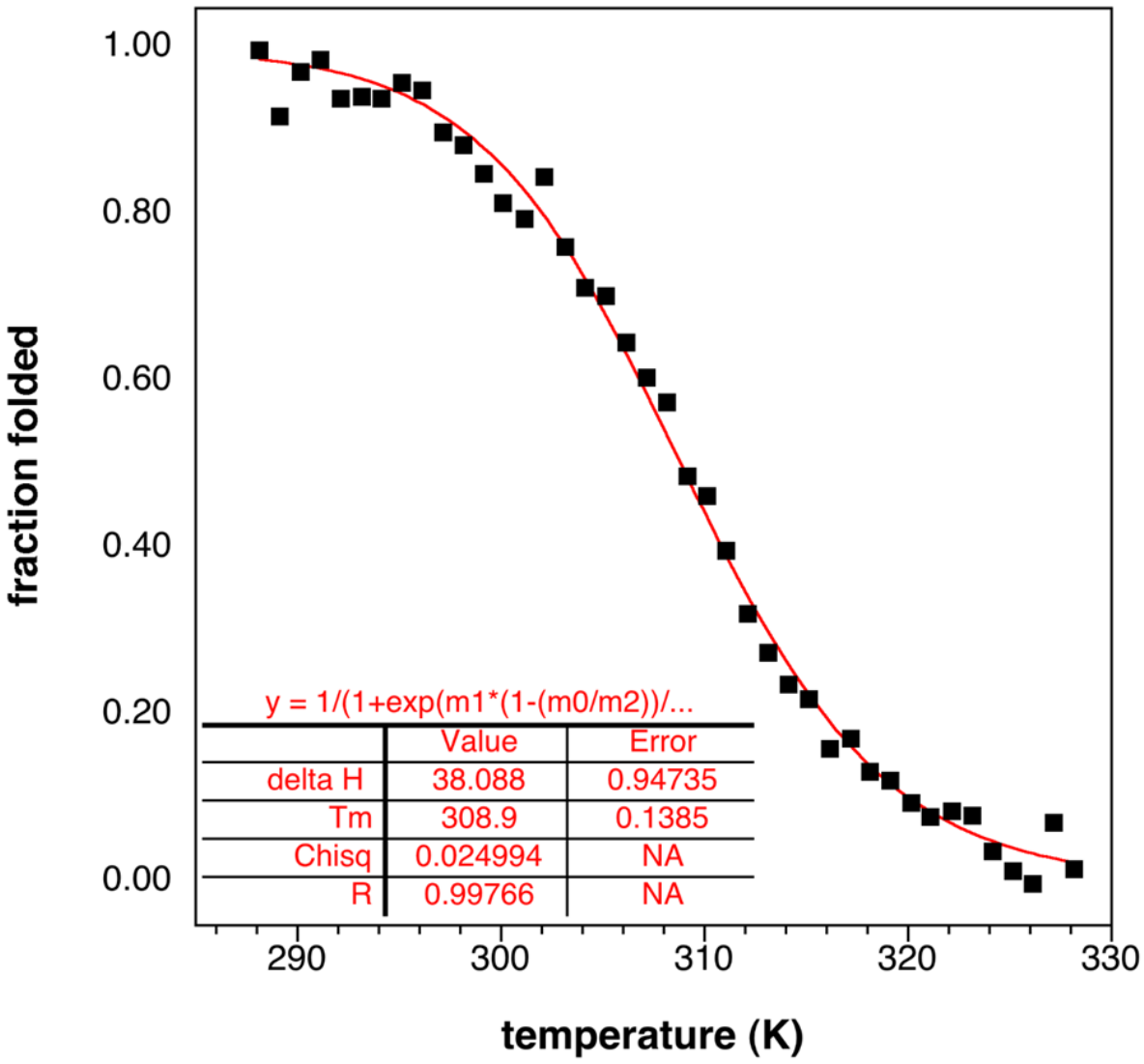

Figure 3.4: Melting Curve of POGH at a 36 °C/hour Ramp.

Results from thermal denaturation studies with the 12 °C/hour ramps suggest that the rate of heating has only modest effect on the measured melting temperatures. Under these conditions of slower warming, preliminary T_m values for HPOG and POGH are 33 °C and 34 °C, respectively.

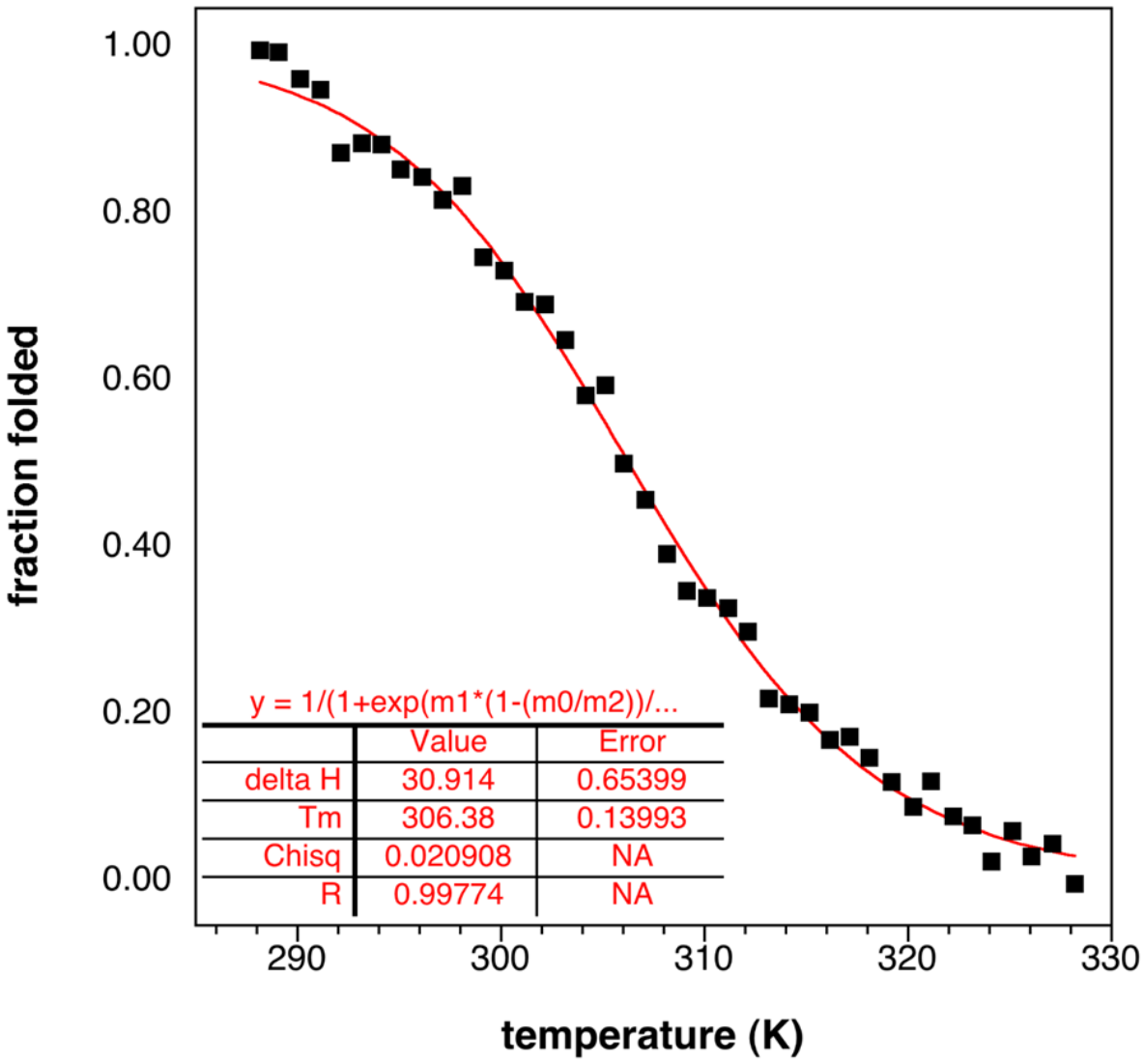

Figure 3.5: Melting Curve of HPOG at a 12 °C/hour Ramp.

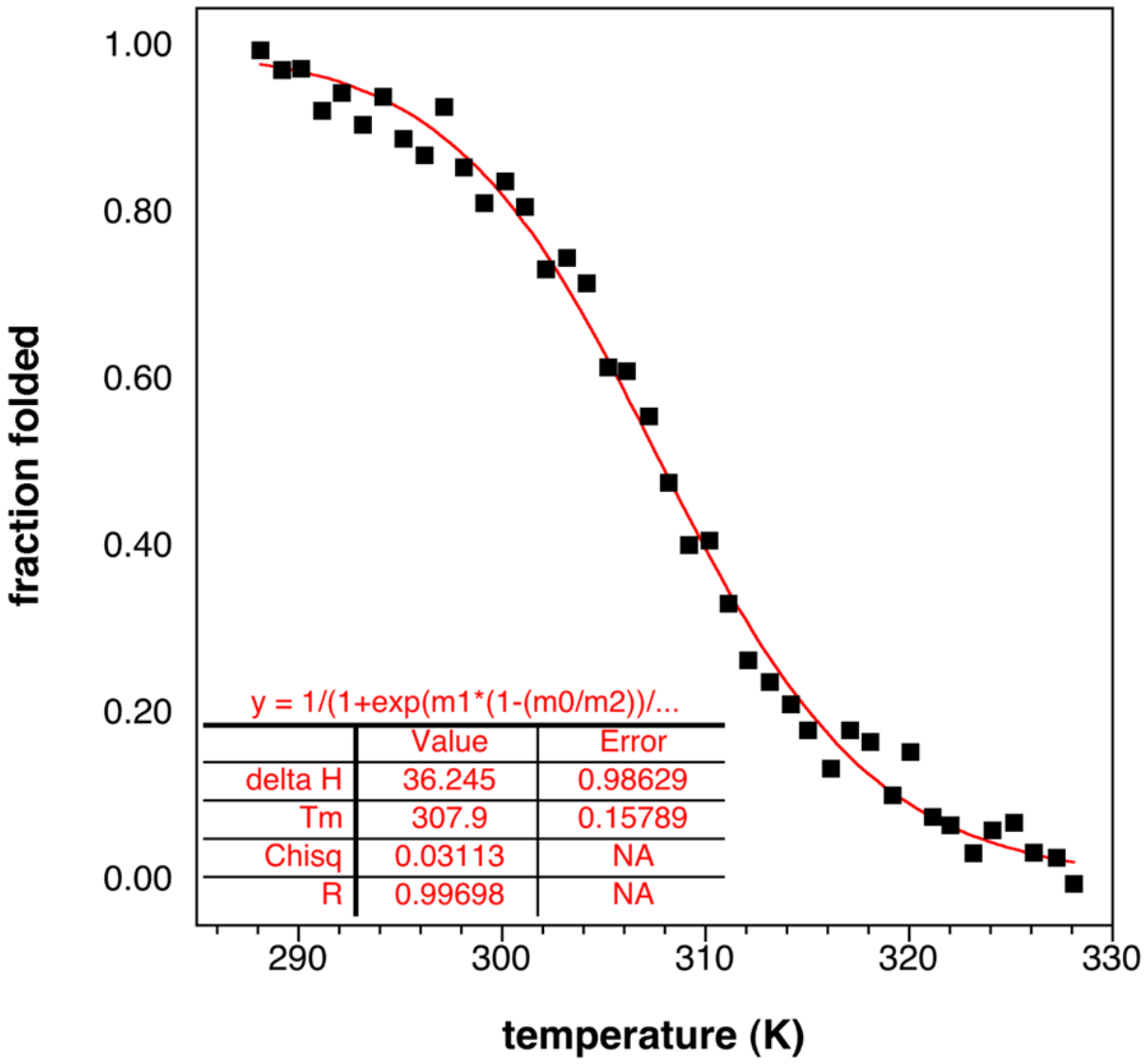

Figure 3.6: Melting Curve of POGH at a 12 °C/hour Ramp.

3.2 *N*-Anchored Complex Studies

Circular dichroism spectroscopy was similarly utilized to study the secondary structure of the novel *N*-Anchored complex. As with the free peptides, the *N*-Anchored material was dissolved in PBS buffer. However, the concentration of complex was 0.067 mM, so that the

total concentration of *strands* was 0.20 mM (i.e., 3 x 0.67 mM). The complex exhibited a maximum at 225 nm at 15 °C, indicative of a triple-helix formation.

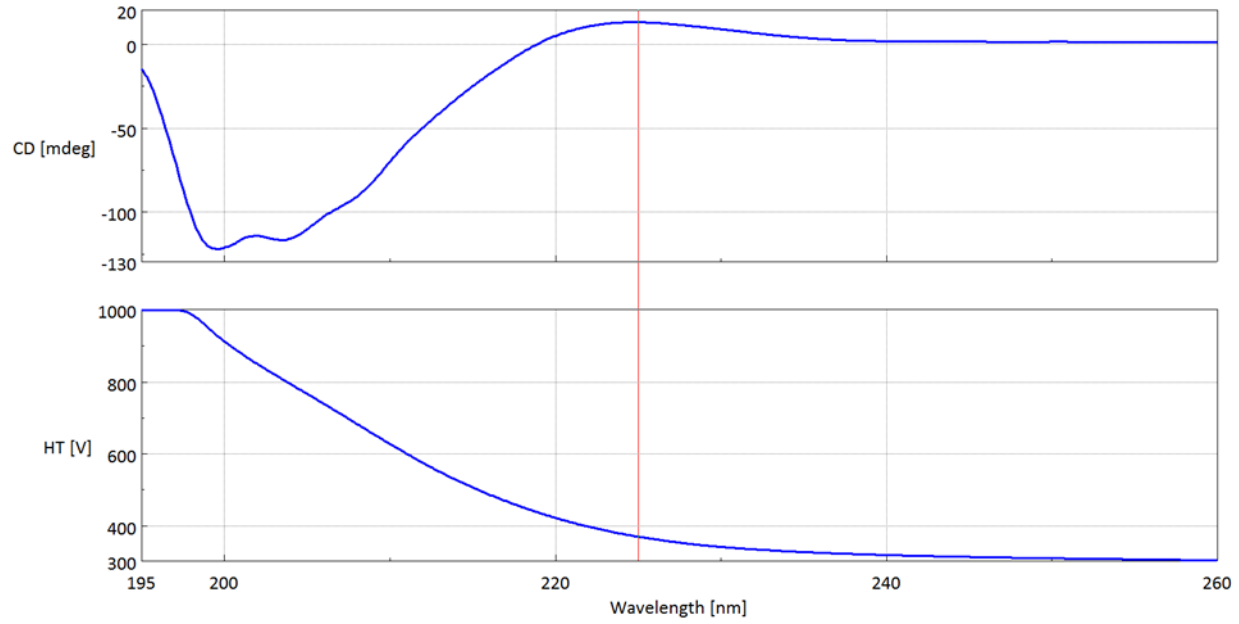

Figure 3.7: CD Spectra of *N*-Anchored HPOG at 15 °C.

Thermal denaturation studies at 36 °C/hour ramps reveal unfolding at a higher temperature. The experimental T_m is 46.3 $\mp$ 2.4 °C, with representative data shown in Figure 3.8. Thus, the presence of the ruthenium anchor (Tp-Ru) at the *N*-termini imparts a degree of overall stabilization, but decreases cooperativity (i.e., the melting curve is more broad). Presumably, by binding the *N*-termini, an initial point of denaturation is eliminated. To date, the precise origin of the cooperativity loss is unknown.

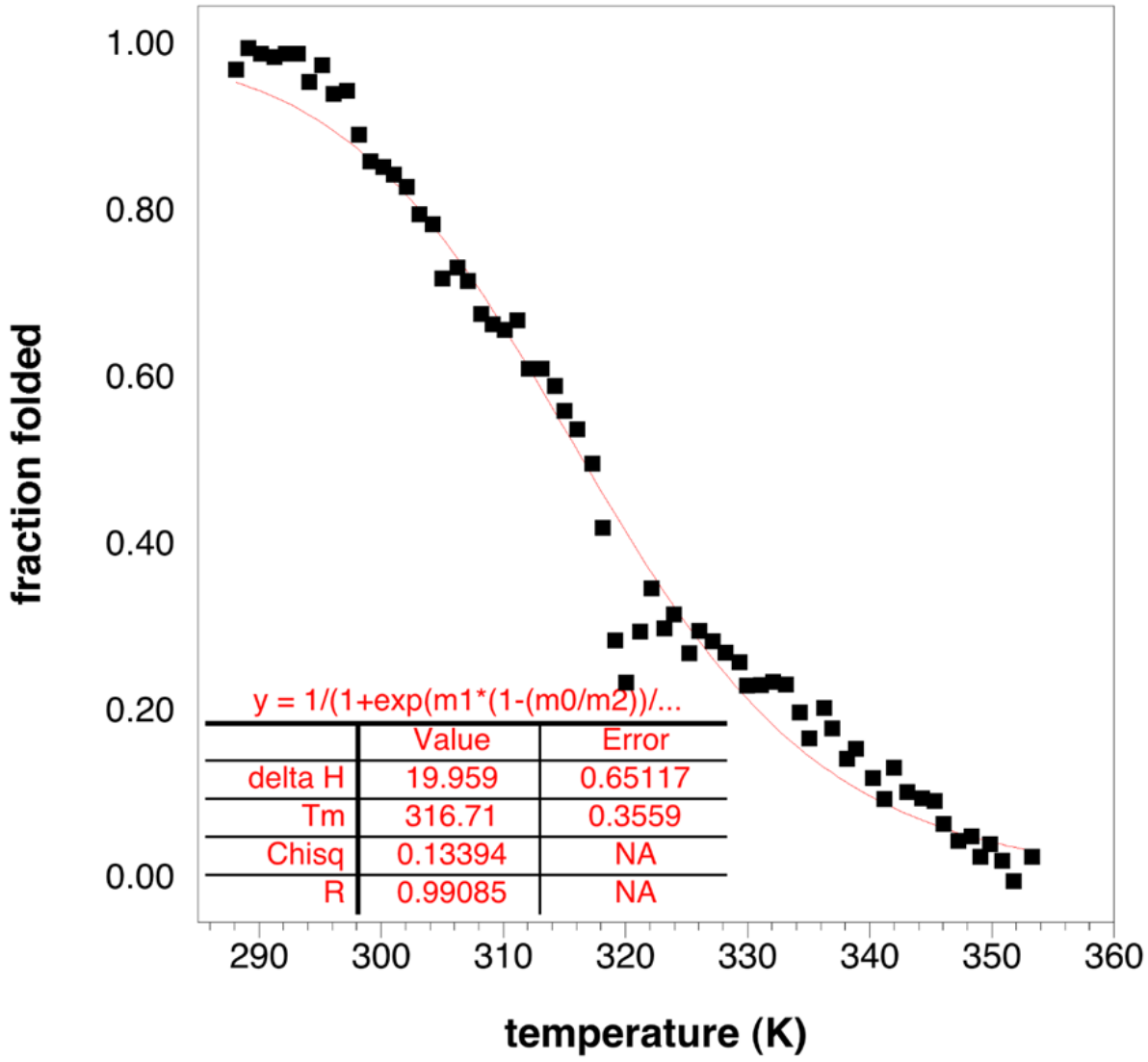

Figure 3.8: Melting Curve of *N*-Anchored HPOG at a 36 °C/hour Ramp.

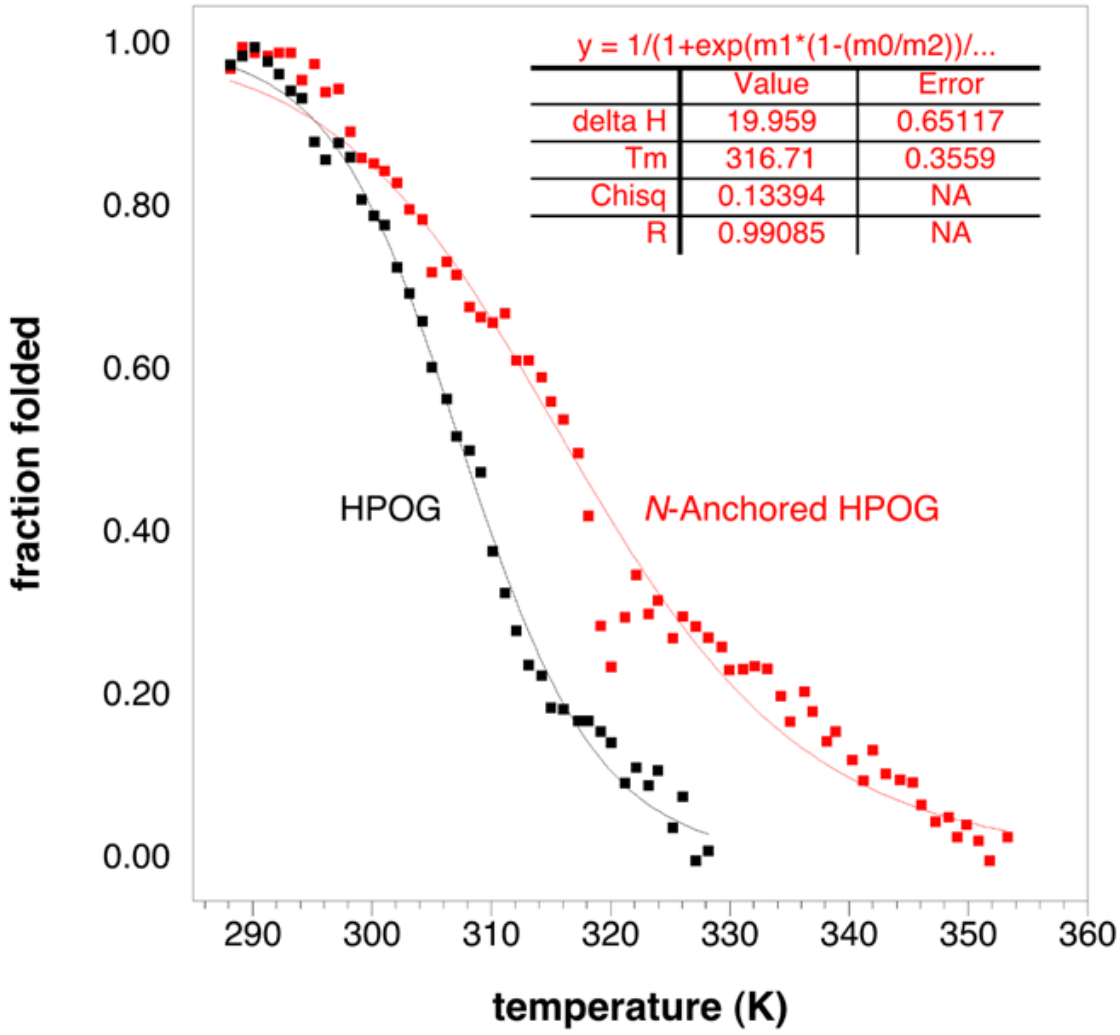

Figure 3.9: Melting Curve Comparisons of HPOG and the *N*-Anchored Complex of HPOG.

CHAPTER 4: CONCLUSIONS

Natural collagen maximizes interstrand hydrogen-bonding. The addition of the link-and-spacer residues, His and Ahx, to collagen analogues with a $(Pro\text{-}Hyp\text{-}Gly)_7$ core is likely to impart conformational mobility, providing a site where fraying of H-nonds (denaturation) can begin. This is illustrated in the lower T_m of HPOG and POGH versus the reported T_m from Chenoweth et

al.[18,19] However, immobilizing the strands onto Tp-Ru locks the three strands in permanent proximity, leading to a greater T_m in the *N*-Anchored system. Thus, Tp-Ru has been found to be a suitable complex to anchor the collagen triple-helix, but this stabilization comes at a cost. Structural distortions may inhibit optimal approach to among peptides, leading to a loss of cooperativity. A longer spacer molecule may address this issue. Computational studies predict anchoring at the *C*-termini will yield a higher melting temperature. The thermal denaturation of this model has yet to be examined.

CHAPTER 5: EXPERIMENTAL

Synthesis of Ac-His-Ahx-(Pro-Hyp-Gly)$_7$-NH$_2$ (HPOG)

The 23-residue molecule was prepared via automated Fmoc-based solid-phase peptide synthesis. Rink Amide MBHA LL resin (0.20 mmol, loading 0.35 mmol/g) was placed in the reaction vessel. Appropriate amino acids (0.80 mmol), HBTU (0.20 mmol), and HOBt (0.20 mmol) were added to plastic vials, which were then capped and loaded into the synthesizer in sequence. HBTU and HOBt were used to activate the carboxyl groups of the amino acids. Double coupling protocols were required for proline; hence duplicate vials were prepared. Acetic anhydride (2.5 mL) was added to the last vial for acetylation of the *N*-terminus. During the synthesis, the protocol dissolved the contents of each vial in DMF/DIPEA solution and transferred the mixture to the reaction vessel. Coupling times were set to 20 minutes. Deprotection was effected using piperidine in DMF.

Upon completion, the reaction vessel was removed from the synthesizer and the contents were isolated on a Hirsch funnel by suction filtration. The loaded resin was rinsed with

glacial acetic acid (~5 mL), dichloromethane (~5 mL), and methanol (~5 mL). The resin was then dried under high vacuum for > 1 hour. The peptide was cleaved from the resin by treatment with of a mixture of TFA (97%), TIPS (1%), anisole (1%), and water (1%) for 4 hours. The resin beads were separated from the cleavage solution using suction filtration, and the filtrate was introduced dropwise into chilled diethyl ether (20 mL). After standing at 4 °C for 24 hours, the suspended peptide was collected by suction filtration on a fine glass fritted funnel, washed with small portions of ether, and dried under high vacuum for 2 hours. The peptide was then dissolved in a minimal amount of 1:1 ACN/H_2O for purification via reversed-phase HPLC. A semi-preparative C18 column (22 x 250 mm, 2 µm particle size) was used, with a linear gradient of 100% water to 100% acetonitrile (160.0 mL, 8.00 mL/min) containing 0.1% TFA. The peak which absorbed at 214 nm with retention time of 10-12 minutes was collected. This peak contains the desired peptide as confirmed by ESI-QTof mass spectrometry (**m/z** for $[M + H]^+$: calculated 2179.04, found 2179.37; for $[M + 2H]^{2+}$: calculated 1090.03, found 1090.77; $[M + 3H]^{3+}$: calculated 727.02, found 727.74). The eluate was lyophilized for storage.

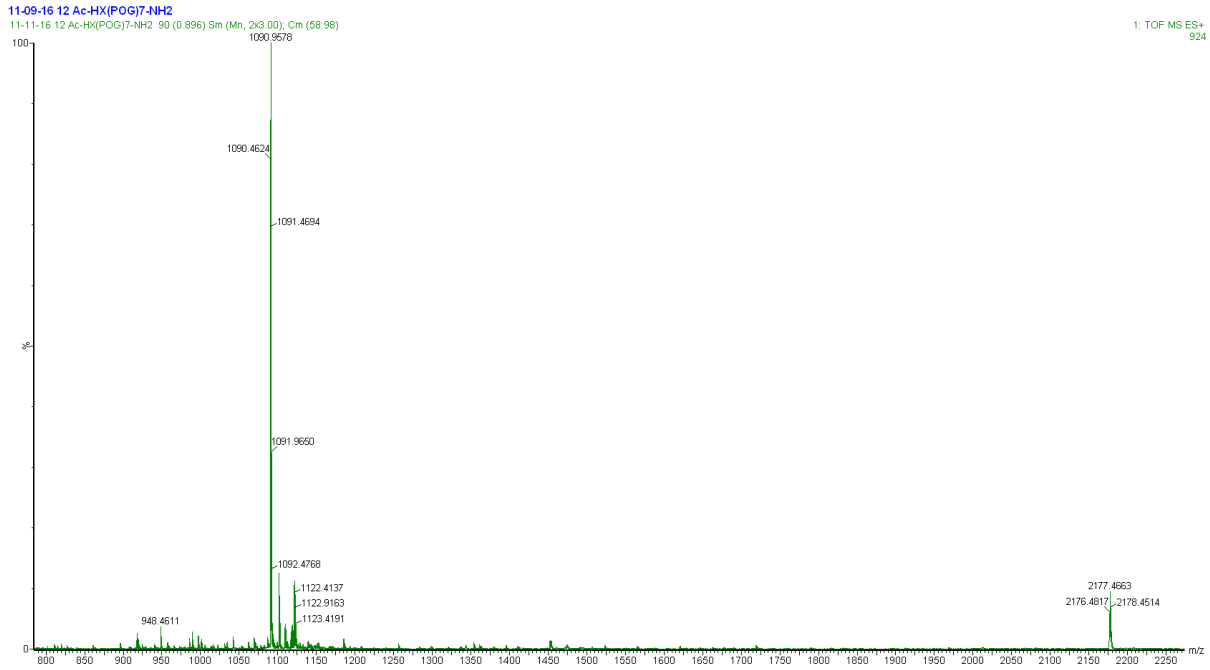

Figure 5.1: ESI+ MS Spectrum of HPOG.

Synthesis of Ac-(Pro-Hyp-Gly)$_7$-Ahx-His-NH$_2$ (POGH)

This compound was prepared in a similar manner to the HPOG isomer, except that 6-aminohexanoic acid and L-histidine were appended at the *C*-terminus. After HPLC, the identity of the peptide was confirmed by ESI-QTof mass spectrometry (**m/z** for $[M + H]^+$: calculated 2179.04, found 2178.87; for $[M + 2H]^{2+}$: calculated 1090.03, found 1090.18).

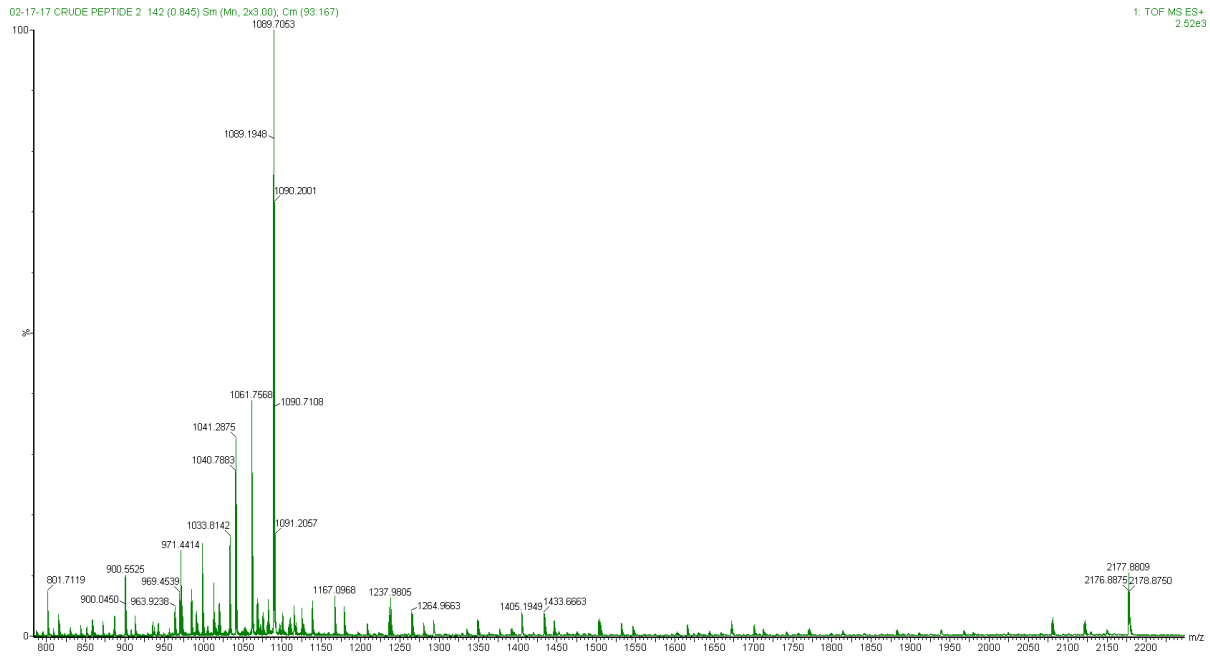

Figure 5.2: ESI+ MS Spectrum of POGH.

Synthesis of tris(pyrazol-1-yl)hydroboratoruthenium(II) (Tp-Ru)

Ruthenium trichloride (1.0 mmol), potassium tri(1-pyrazolyl)borohydride (1.0 mmol) and potassium iodide (0.1 mmol) were added to a 50-mL round-bottom flask. Acetonitrile (10 mL) was added into the flask to mix the contents. The mixture was deoxygenated with a gentle stream of nitrogen, then heated under reflux (~80 °C) for 45 minutes. After cooling to room temperature, dichloromethane (5 mL) was added. The mixture was filtered by gravity, and the green filtrate was dried using rotary evaporation. A portion of this crude Ru(III) material (0.25 mmol) and sodium ascorbate (0.25 mmol) were added into a 50-mL round-bottom flask. Acetonitrile (10 mL) and water (2 mL) were added to mix the contents. The mixture was heated to 40 °C for 45 minutes, during which time the color changed to light yellow/tan. The mixture was then purified via RP-HPLC on a C18 column (22 x 250 mm, 2 µm), using a linear gradient of

100% water to 100% acetonitrile (160.0 mL, 8.00 mL/min). The largest peak that absorbed at 360 nm was collected (11-14 min retention time). The eluate was lyophilized to a sticky gold solid for storage.

Synthesis of *N*-Anchored Complex

The HPOG peptide (0.035 mmol) and Tp-Ru (0.01 mmol) were dissolved in 3.0 mL of 95% ethanol. The mixture was initially heated to 60 °C for 24 hours. Analytical-scale HPLC showed little conversion had taken place, so a small amount of DIPEA (10 µL) and water (3 mL) were added to the mixture to assist dissolution. Once solution formed, heating continued at 60 °C for 48 hours.

The solution (~6 mL) was purified through RP-HPLC on a C18 column (22 x 250 mm, 2 µm), using a linear gradient of 100% water to 100% acetonitrile (160.0 mL, 8.00 mL/min). The one observed peak was collected (360 nm, 15-16 min retention time). The eluate was lyophilized for storage. Once solidified, the contents were dissolved in DMSO-d_6 for proton NMR confirmation.

Preparation of 0.20 mM PBS Solution

Using a 1-L volumetric flask, NaCl (8.00 g), Na_2HPO_4 (2.16 g), KCl (0.20 g), and KH_2PO_4 (0.20 g) were dissolved in deionized water (1.00 L). The flask was sonicated to ensure dissolution.

Mass Spectrometry Setup

Mass spectra were acquired on Micromass Q-ToF Micro mass spectrometer with an electrospray ionization source. The samples were dissolved (1:1 ACN/H_2O & 0.1% formic acid) and spectra were obtained over a 200 – 2500 **m/z** range. Parameters were set as follows: injection volume (1 mL), ion mode (positive), flow rate (20 µL/min), source temperature (90 °C), desolvation temperature (140 °C), capillary voltage (2700 V), sample cone voltage (30 V), extraction cone voltage (2 V), cone flow (20 L/hour), and desolvation flow (500 L/hr).

Nuclear Magnetic Resonance Setup

Proton NMR spectra were acquired on Bruker AVANCE400 spectrometer. Samples were diluted in DMSO-d_6. 64 scans were used per collection. Proton shifts at approximately 8.95 and 8.35 ppm were investigated.

Circular Dichroism Setup

Circular dichroism experiments closely followed the conditions described by Chenoweth et al. to facilitate comparison of data.[18,19] CD spectra were acquired on Jacso 815 CD spectrometer. Sample preparation for thermal denaturation studies included HPOG, POGH, and the *N*-Anchored complex. Each material was dissolved in PBS solution. Concentrations were estimated by UV-Vis measurement. Both collagen analogues were dissolved to concentration of 0.20 mM solution by diluting accordingly. The *N*-Anchored complex was diluted to approximately 0.067 mM, such that the concentration of peptide strands would equal 0.20 mM. All samples were incubated at 4 °C for 24 hours prior to measurements, to ensure maximal triple-helical formation.

Using a quartz cuvette (0.1 mm path length), spectra were obtained over the 240 to 195 nm range. The wavelength that gave the highest positive signal, 225 nm, was monitored as a function of time in the thermal denaturation experiments.[21,22] The equilibration time between temperature jump and data acquisition was 60 seconds. The temperature ramps were individually assigned (36 °C/hour and 12 °C/hour) and the ellipticity was recorded for every 1°C. The collected data were fit to a two-state model as reported by Vargas-Uribe et al.[20]

REFERENCES

1. Anfinsen, C. B. *Science*. **1973**. 181. 223-228.
2. Pauling, L., Corey, R. B., *Nature*. **1951**, 168, 550-555.
3. Srinivasan, R., Rose, G. D., *Proc. Natl. Acad. Sci. U.S.A*. **1999**. 96, 14258-14267.
4. Ricard-Blum, S. The Collagen Family. *Cold Spring Harb Perspect Biol*. **2011**, 201. 1-16.
5. Watson, J. D., Crick, F. H. C., *Nature*. **1953**, 171, 737-742.
6. Astbury, W.T., Bell, F.O. *Nature.* **1940**. 145. 421–422.
7. Pauling L., Corey R.B. *Proc. Natl. Acad. Sci. USA*. **1951**. 37. 272–281.
8. Ramachandran, G.N. Kartha, G. *Nature*. **1954**. 174. 269–270.
9. Rich, A., Crick F.H.C. *Nature* **1955**. 176. 915–916.
10. Newberry, R.W., VanVeller, B., Raines, R.T. *Chem. Commun*. **2015.** 51. 9624-9636.
11. Grant, M.E. *International Journal of Experimental Pathology*. **2007**. 88. 203–214.

12. Huber, M. et al. *Acta Biomaterialia.* **2009**. 5, 172-180.

13. Muller, R. et al. *Biomaterials*. **2005**. 26. 6962-6972.

14. Chaiko, E.L. *J. Am. Chem. Soc.* **2007**. 129. 14780-14787.

15. Patino M.G. et al., *J. Oral Implantology*. **2002**. 28(5), 220-225.

16. Raines, R.T., et al. *Annu Rev Biochem.* **2009**, 78, 929-958.

17. Raines, R.T. *J Biol. Chem.* **2011**. 286(26). 22905–22912.

18. Chenoweth, D.M. et al. *J. Am. Chem. Soc.* **2015**. 137. 12422-12425.

19. Chenoweth, D.M., et al. *J. Am. Chem. Soc.* **2016**. 138. 9751-9754.

20. Vargas-Uribe M., et al. *J. Membrane Biol*. **2014.** 248(3). 383-394.

21. Kelly, S.; Price, N. *Curr. Protein Pept. Sc.* 2000. *1*. 349-384.

22. Wallace, B. A. *Protein Science*. **2014**. 23. 1765-1772.